Aging Cell (2011) **10,** pp798–806 Doi: 10.1111/j.1474-9726.2011.00720.x

Cellular senescence increases expression of bacterial ligands in the lungs and is positively correlated with increased susceptibility to pneumococcal pneumonia

Pooja Shivshankar,[1] Angela R. Boyd,[1] Claude J. Le Saux,[2] I-Tien Yeh[3] and Carlos J. Orihuela[1]

[1]Department of Microbiology and Immunology, [2]Department of Medicine, Division of Cardiology, and [3]Department of Pathology, The University of Texas Health Science Center at San Antonio, 7703 Floyd Curl Drive, San Antonio, Texas, 78229, USA

Summary

Cellular senescence is an age-associated phenomenon that promotes tumor invasiveness owing to the secretion of proinflammatory cytokines, proteases, and growth factors. Herein we demonstrate that cellular senescence also potentially increases susceptibility to bacterial pneumonia caused by *Streptococcus pneumoniae* (the pneumococcus), the leading cause of infectious death in the elderly. Aged mice had increased lung inflammation as determined by cytokine analysis and histopathology of lung sections. Immunoblotting for p16, pRb, and mH2A showed that elderly humans and aged mice had increased levels of these senescence markers in their lungs vs. young controls. Keratin 10 (K10), laminin receptor (LR), and platelet-activating factor receptor (PAFr), host proteins known to be co-opted for bacterial adhesion, were also increased. Aged mice were found to be highly susceptible to pneumococcal challenge in a PsrP, the pneumococcal adhesin that binds K10, dependent manner. *In vitro* senescent A549 lung epithelial cells had elevated K10 and LR protein levels and were up to 5-fold more permissive for bacterial adhesion. Additionally, exposure of normal cells to conditioned media from senescent cells doubled PAFr levels and pneumococcal adherence. Genotoxic stress induced by bleomycin and oxidative stress enhanced susceptibility of young mice to pneumonia and was positively correlated with enhanced p16, inflammation, and LR levels. These findings suggest that cellular senescence facilitates bacterial adhesion to cells in the lungs and provides an additional molecular mechanism for the increased incidence of community-acquired pneumonia in the elderly. This study is the first to suggest a second negative consequence for the senescence-associated secretory phenotype.

Key words: cellular senescence; aging; SASP; age-associated inflammation; infectious disease; pneumonia.

Introduction

Pneumonia is the leading cause of infectious death among the elderly (Lopez *et al.*, 2006). Risk factors for community-acquired pneumonia (CAP) include advanced age, underlying morbidities, and the presence of chronic low-grade inflammation (Lexau *et al.*, 2005; Yende *et al.*, 2005). Chronic inflammation is a risk factor for CAP as it results in increased laminin receptor (LR) and platelet-activating factor receptor (PAFr) protein levels on the surface of host cells (Cundell *et al.*, 1995; Hinojosa *et al.*, 2009; Orihuela *et al.*, 2009). LR and PAFr are in turn co-opted by *Streptococcus pneumoniae*, *Haemophilus influenzae*, *Neisseria meningitidis,* and other respiratory tract pathogens for host cell adhesion and bacterial translocation across the alveolar-capillary and blood–brain barriers (Cundell *et al.*, 1995; Swords *et al.*, 2000; Barbier *et al.*, 2008; Orihuela *et al.*, 2009). In support of a strong link between age-associated inflammation and severe pneumonia, it has been previously shown that healthy aged mice express elevated levels of PAFr in their lungs (Hinojosa *et al.*, 2009). Moreover, young mice infused for 5 days with physiologically age-relevant levels of tumor necrosis factor α (TNFα) had elevated levels of lung PAFr and were more susceptible to pneumococcal pneumonia with 100-fold more bacteria in their lungs than saline controls 2 days postchallenge (Hinojosa *et al.*, 2009).

Cellular senescence is an age-associated phenomenon whereby cells with shortened telomeres or those that have undergone DNA damage (i.e., genotoxic stress) lose the capacity to replicate without undergoing apoptosis. This is the result of activation of the p53-p21 and p16-pRb tumor suppressor pathways (Campisi & d'Adda di Fagagna, 2007). Cellular senescence has paradoxically been implicated as a tumor-suppressive mechanism owing to cell cycle arrest, as well as a promoter of tumor invasiveness due to the senescence-associated secretory phenotype (SASP) which includes the production and secretion of proinflammatory cytokines Interleukin (IL)-1α, IL-6 and IL-8, proteases, and assorted growth factors (Coppe *et al.*, 2009). Pertinent to this investigation, proliferation of epithelial cells has also been shown to be modulated by cytokeratin 10 (K10) (Paramio *et al.*, 1999). During terminal differentiation, K10-induced inhibition occurs through pRb as a result of sequestration and phosphorylation of AKT that consequently impedes pRb phosphorylation and leads to cell cycle arrest (Paramio *et al.*, 2001). Coincidently, surface-exposed K10 has been demonstrated to serve as a bacterial ligand for the *S. pneumoniae* adhesin PsrP on lung cells and for the *Staphylococcus aureus* adhesin ClfB within the nares (O'Brien *et al.*, 2002; Shivshankar *et al.*, 2009).

The presence of senescent cells in the lungs of healthy aged animals has recently been demonstrated by Kreiling *et al.* using the new senescence marker histone macro H2A (mH2A) (Kreiling *et al.*, 2011). Other investigators have also reported an age-dependent accumulation of senescent cells in skin, liver, atherosclerotic lesions, muscle, and other tissues (Krtolica & Campisi, 2002; Campisi, 2005; Campisi & d'Adda di Fagagna, 2007). Importantly, studies have identified p16-positive senescent cells in the lungs of individuals with chronic obstructive pulmonary disease (COPD), and they are thought to exacerbate pathology owing to their proinflammatory phenotype (Garcia *et al.*, 2007; Aoshiba & Nagai, 2009; Tsuji *et al.*, 2010). Both COPD and advanced age are established risk factors for CAP (Lexau *et al.*, 2005).

Given the documented presence of senescent cells in aged tissues, the proinflammatory phenotype of senescent cells, and the fact that

Correspondence
Carlos J. Orihuela, Department of Microbiology and Immunology, The University of Texas Health Science Center at San Antonio, 7703 Floyd Curl Drive, San Antonio, Texas 78229-3900, USA. Tel.: (210) 567-3973; fax: (210) 567-6612; e-mail: orihuela@uthscsa.edu

Accepted for publication *28 April 2011*

inflammation is a risk factor for CAP as a result of increased ligand expression in the lungs, we hypothesized that cellular senescence enhances susceptibility to pneumococcal pneumonia through increased bacterial ligand expression. In this study, we therefore tested young and aged mice for the levels of senescence markers in their lungs, assessed whether senescent lung cells expressed elevated levels of the pneumococcal ligands K10, LR, and PAFr *in vitro* and *in vivo*, tested for a paracrine effect of SASP on bacterial adhesion, and determined whether genotoxic stress increased susceptibility to pneumococcal infection.

Results

Age-associated inflammation occurs in the lungs of healthy aged animals and is positively correlated with increased levels of senescence markers

Consistent with the concept of age-associated inflammation, lung homogenates from healthy aged (19–22 month) mice had increased levels of the proinflammatory cytokines IL-1α, IL-1β, IL-6, TNFα, and CXCL1 vs. those obtained from young (4–5 month) animals (Fig. 1A). Likewise, histological examination of lung sections from the same animals showed that aged mice had an increased incidence of interstitial and peribronchial inflammation (Fig. 1B,C). In agreement with the findings by Kreiling *et al.* showing that senescent cells are present in the lungs of healthy aged C57Bl/6 mice (Kreiling *et al.*, 2011), in both human and Balb/cBy mouse lung samples, we observed an age-dependent increase in the senescence markers p16 and pRb by Western blot (Fig. 2). For mature (51–63 year) and aged (64–82 year) humans, we also observed increased levels of mH2A vs. younger controls (43–50 year). Thus, the proinflammatory cytokine profile observed in healthy aged mice was correlated positively with elevated p16 and pRb levels. These findings support the concept that cellular senescence occurs in the aged lungs and acts as a source of inflammation.

Pneumococcal ligands are elevated in aged lungs and contribute to the enhanced susceptibility to pneumonia

As indicated, *S. pneumoniae* binds to the host proteins K10, LR, and PAFr on lung cells (Cundell *et al.*, 1995; Orihuela *et al.*, 2009; Shivshankar *et al.*, 2009). Western blot analyses of whole-lung homogenates from young, mature, and aged human lung biopsy samples demonstrated an age-dependent increase in LR and PAFr, with a trend for K10 in young vs. aged samples ($P = 0.17$) (Fig. 3A). Aged mice showed a statistically significant increase in all three ligands vs. young controls (Fig. 3B). Immunohistochemistry of mouse lung sections confirmed these observations for K10 with intense staining for both the alveolar and bronchial epithelial cells but not endothelial cells or fibroblasts surrounding the bronchi of aged mice vs. young controls (Fig. 3C).

An important role for elevated K10 during pneumococcal pneumonia in aged mice was confirmed by challenging young and aged animals with wild-type bacteria or with an isogenic mutant deficient in PsrP (Δ*psrP*) (Rose *et al.*, 2008). Not only was mortality in aged mice PsrP-dependent (Fig. 4A), but 2 days after challenge aged mice infected with the wild-type strain had median bacterial titers in their lungs and blood 10- and 240-fold greater, respectively, than those infected with the mutant strain (Fig. 4B). Thus, we determined that increased K10, LR, and PAFr expression occurred in the lungs of aged humans and mice. Furthermore, aged mice were more susceptible to pneumococcal infection in a PsrP/K10-dependent manner.

Senescent lung epithelial cells express K10 and LR

We subsequently tested whether induction of cellular senescence resulted in elevated K10, LR, and PAFr production by lung epithelial cells. *In vitro* treatment of A549 human type II pneumocytes with bleomycin resulted in cellular senescence. Indeed, we observed the expected phenotypic changes such as cell flattening, increased senescence-associated

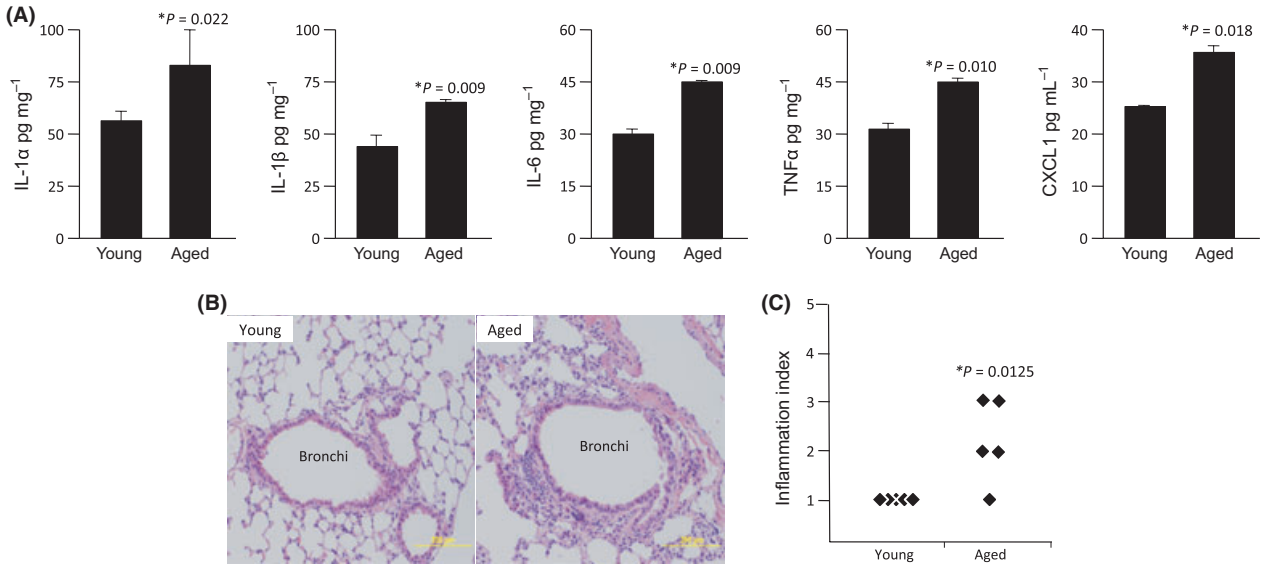

Fig. 1 Aged mice experience low-grade lung inflammation. (A) Levels of IL-1α, IL-1β, IL-6, TNFα, and CXCL1 in whole-lung homogenates from healthy young (4–5 month, $n = 5$) and aged (19–21 month, $n = 5$) female Balb/cBy mice were assessed by ELISA. (B) Representative micrographs of Hematoxylin- and Eosin-stained lung sections from the same animals. Note the enhanced interstitial and peribronchial inflammation in the aged lung section. (C) Scoring of lung inflammation in the same lung sections (1 is no pathology on histological cross-section, and 5 is extensive cellular infiltration, edema, and alveolar consolidation). Each diamond indicates the blinded pathological score for an individual mouse. In panels A and C, asterisks denote a statistical significant difference when using a two-tailed Student's *t*-test.

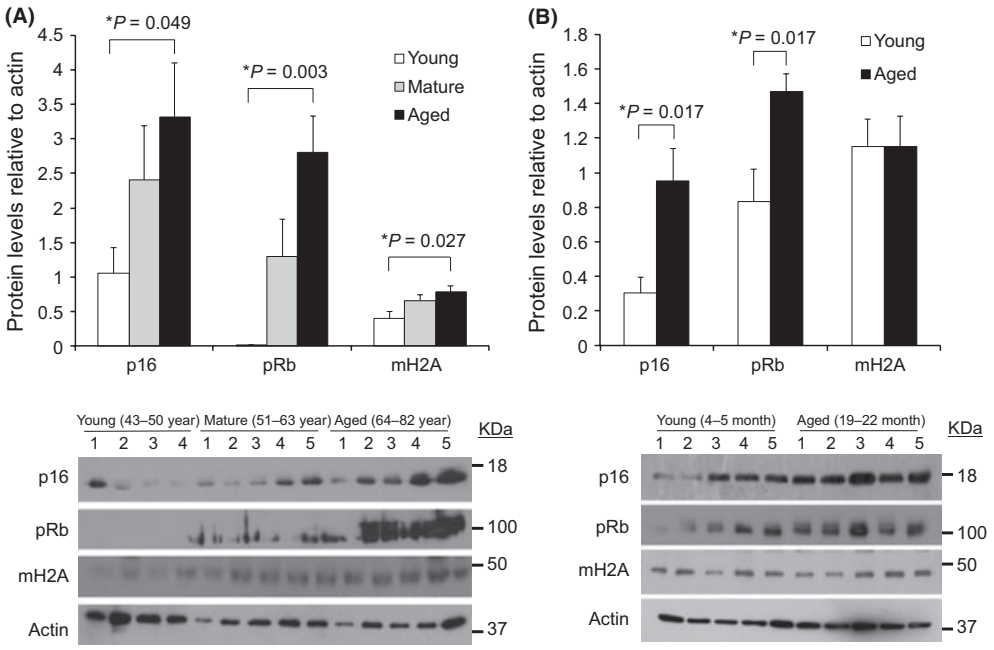

Fig. 2 Aging is associated with increased expression of senescence markers in the lungs. (A) Densitometric analyses and representative Western blots for the senescence markers p16, pRb, and mH2A in tissue lysates from lung biopsies obtained from young (43–50 years; $n = 4$), mature (51–64 years; $n = 5$), and aged (65–82 years; $n = 5$) humans. (B) The same analyses were performed using whole-lung homogenates obtained from young (4–5 months; $n = 5$) and aged (19–22 months; $n = 5$) female Balb/cBy mice. For panels A and B, histograms show composite densitometric data (protein/actin) with actin probed from the same lanes and membrane as the tested protein. The representative actin blot shown corresponds to the p16 immunoblot. Statistical significance was determined using a two-tailed Student's *t*-test.

β-galactosidase activity, and elevated expression of p16, pRb, and mH2A along with a decline in phospho-pRb by immunoblotting (Fig. 5A,B). Induction of senescence with bleomycin resulted in a dose-dependent increase in the expression of K10 and LR, but not PAFr (Fig. 5B). Subsequently, immunofluorescence assay confirmed nuclear accumulation of pRb simultaneous to increased K10 expression in bleomycin-treated cells but not in controls (Fig. 5C). Finally, bacterial adhesion assays demonstrated that senescent cells were more permissive for infection with a 3- to 5-fold increase in the number of attached wild-type but not PsrP-deficient pneumococci to senescent cells when compared to normal cells (Fig. 5D,E). Thus, induction of cellular senescence in lung cells was associated with increased expression of two pneumococcal ligands and increased permissiveness for bacterial attachment.

SASP enhances permissiveness of normal cells for infection

PAFr and LR have been shown to be upregulated by lung cells following exposure to proinflammatory cytokines (Cundell *et al.*, 1995; Orihuela *et al.*, 2009). Thus, it is possible that SASP enhances bacterial ligand expression on presenescent normal lung cells in a paracrine manner. *In vitro*, we confirmed that bleomycin-induced senescent A549 cells increased intracellular IL-1α levels but that it was not secreted (Fig. 6A). Further, senescent cells secreted increased amounts of IL-6 and IL-8 but did not produce IL-1β, TNFα, IL-10, or IL-12 (Fig. 6A). Normal A549 cells exposed to conditioned media from senescent cells for 2 h presented a 2.2-fold increase in bacterial adhesion compared to cells exposed to conditioned media from normal cells (Fig. 6B). Finally, treatment of A549 cells with senescent media resulted in no changes in K10 or LR, but resulted in a doubling of PAFr levels after 2 h (Fig. 6C). The latter remained constant through 4 and 6 h of incubation with conditioned media (data not shown).

Genotoxic stress enhances susceptibility of young mice to pneumonia

Finally, we tested whether administration of agents known to cause DNA damage enhanced bacterial ligand expression and susceptibility to pneumonia. Genotoxic stress in young mice was induced either by intratracheal administration of bleomycin once (0.033 mg kg^{-1} body weight) or supplementation of drinking water with 0.5% hydrogen peroxide for 3 weeks. The latter causes DNA damage through oxidative stress (Weiner *et al.*, 2000). In mice administered bleomycin and hydrogen peroxide we observed dramatic changes in lung histology and high levels of IL-1α, IL-1β, IL-6, CXCL1, and TNFα (Fig. S1). Both bleomycin- and hydrogen peroxide-treated mice were highly susceptible to pneumococcal infection vs. saline-administered controls. Two days postchallenge, bleomycin- and hydrogen peroxide-treated mice had 10- to 100-fold more bacteria in their lungs and bloodstream than their respective controls (Figure 7A). Levels of p16, pRb, and LR were elevated in the lungs of genotoxic stressed mice, whereas mH2A, K10, and PAFr were unchanged (Figure 6B). Thus, administration of genotoxic agents had pleiotropic effects that included significant changes in lung structure along with increased expression of senescence markers and susceptibility to bacterial infection.

Discussion

Advanced age is an established risk factor for CAP (Lexau *et al.*, 2005), with more than 800 million people worldwide greater than 65 years of age (Kinsella & Velkoff, 2001). Overlapping with this, 210 million adults have COPD worldwide (WHO 2009), a condition associated with and exacerbated by cellular senescence that is also a risk factor for CAP (Lexau *et al.*, 2005; Aoshiba & Nagai, 2009). Thus, close to 1 billion adults worldwide are at risk for pneumonia. Our finding that senescent lung

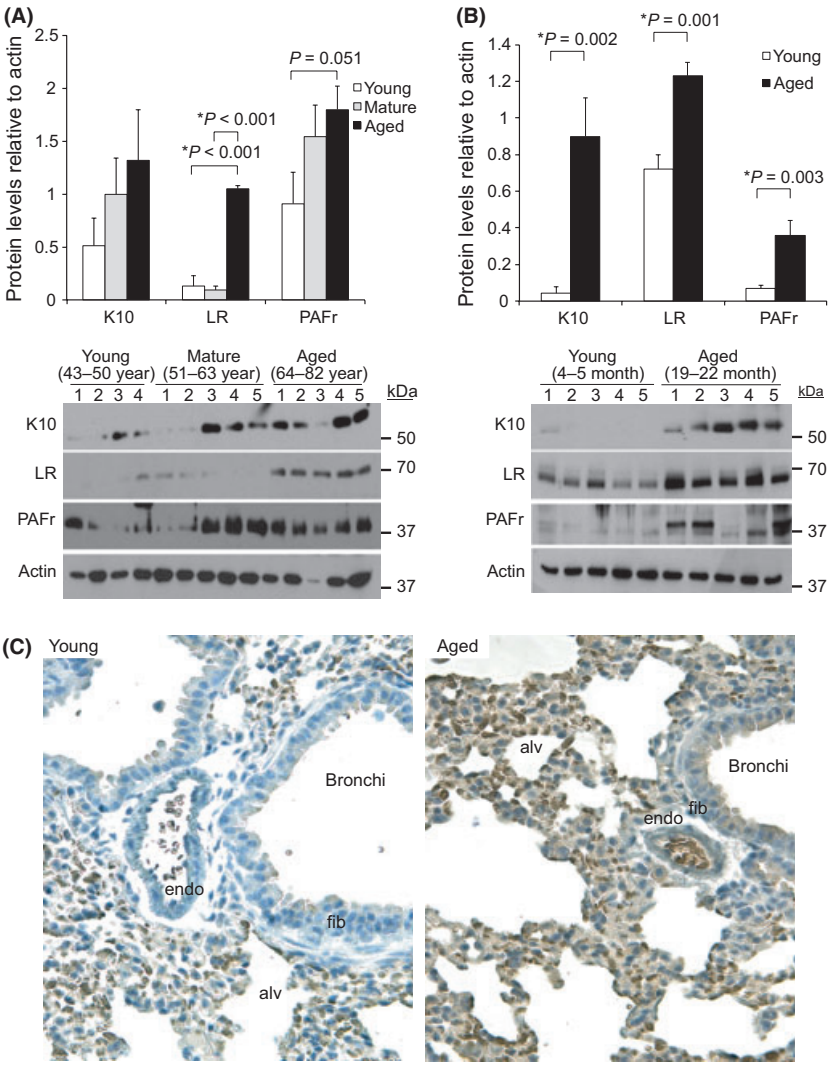

Fig. 3 Aging is associated with increased bacterial ligand expression in the lungs. (A) Densitometric analyses and representative Western blots for the pneumococcal ligands K10, laminin receptor (LR), and PAFr in tissue lysates from lung biopsies obtained from young (43–50 years; $n = 4$), mature (51–64 years; $n = 5$), and aged (65–82 years; $n = 5$) humans. (B) The same analyses were performed using whole-lung homogenates obtained from young (4–5 months; $n = 5$) and aged (19–22 months; $n = 5$) female Balb/cBy mice. For panels A and B, histograms show composite densitometric data (protein/actin) with actin probed from the same lanes and membrane as the tested protein. The representative actin blot shown corresponds to the LR immunoblot. Statistical significance was determined using a two-tailed Student's *t*-test. (C) Representative micrographs of young and aged mouse lung sections immunohistochemically stained for K10. Note that in aged mice, K10 is expressed at high levels in alveolar (alv) and bronchial epithelial cells but remains low in the vascular endothelium (endo) and fibroblasts (fib) surrounding the bronchi.

cells have increased levels of K10 and LR, and can induce the expression of PAFr on normal cells, potentially helps to explain why the elderly and individuals with COPD are predisposed for CAP. Specifically we have demonstrated that senescent cells, normal cells exposed to senescent-conditioned media, aged mice, and young mice exposed to genotoxic stress were more permissive for bacterial adhesion and susceptible to pneumococcal pneumonia, respectively.

The age-associated increase in inflammation that we observed in the lungs of healthy aged mice was consistent with prior publications that have shown elevated levels of IL-6, IL-8, and neutrophils within the lungs of healthy elderly human volunteers (Meyer *et al.*, 1996, 1998). Likewise, they were consistent with the reported SASP profile for senescent HeLa cells (Coppe *et al.*, 2008) and that observed herein for senescent lung epithelial cells. Our observation that elderly humans and aged mice had enhanced levels of p16 and pRb were also in agreement with those by others demonstrating elevated levels of senescent cells in the lungs of aged mice and elevated senescence markers in multiple tissues from aged animals (Campisi, 2005; Kreiling *et al.*, 2011). Thus, considerable evidence now exists that cellular senescence occurs in the aged lungs and that it contributes to the observed age-associated inflammation. Notably, although increased for humans, levels of mH2A were not increased in the lungs of 19- to 22-month (i.e., aged) Balb/cBy mice when examined by Western blot. This was in contrast to that observed by Kreiling *et al.* in C57Bl/6 mice but may be owing to the fact that they examined 36-month-old animals (Kreiling *et al.*, 2011).

Bacterial attachment to lung cells is a requisite event in the pathogenesis of pneumonia (Kline *et al.*, 2009; Paterson & Orihuela, 2010). This is particularly true for the encapsulated extracellular respiratory tract pathogens such as *S. pneumoniae* (Orihuela *et al.*, 2005). Yende *et al.* and our own studies have shown elevated levels of IL-6 and TNFα are risk factors for CAP as a result of enhanced bacterial ligand expression (Yende *et al.*, 2005; Hinojosa *et al.*, 2009). PAFr serves as a ligand for *S. pneumoniae*, *Haemophilus influenzae,* and *Pseudomonas aeruginosa* as well as many other bacteria that have surface-exposed phosphorylcholine on their surface (Cundell *et al.*, 1995; Swords *et al.*, 2000; Barbier *et al.*, 2008). LR serves as a ligand for *H. influenzae* and *Neisseria meningitidis* (Orihuela *et al.*, 2009). K10 is also a ligand for PsrP from *S. pneumoniae* and ClfB of *Staphylococcus aureus* (O'Brien *et al.*, 2002; Shivshankar *et al.*, 2009). Respiratory tract pathogens also bind to other inflammation-regulated proteins such as intercellular adhesion molecule 1 (ICAM-1) and carcinoembryonic antigen-related cell adhesion molecule 1 (CEACAM1) that were not tested but are also most likely upregulated as a result of age-associated inflammation (Avadhanula *et al.*, 2006; Conners *et al.*, 2008). Thus, the enhanced expression of bacterial ligands on either senescent

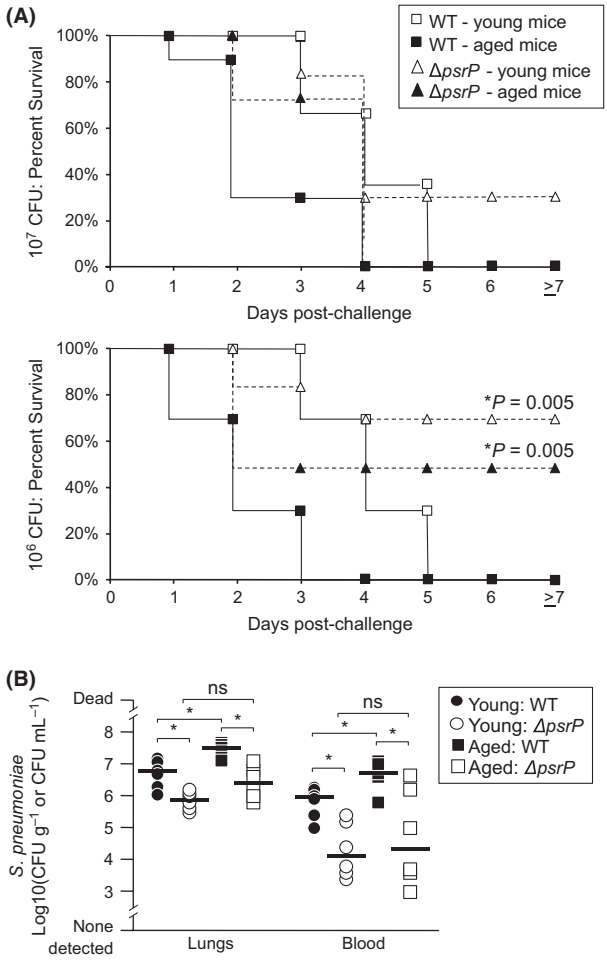

Fig. 4 Aging enhances susceptibility to pneumococcal pneumonia in a K10-dependent manner. (A) Kaplan–Meier plot demonstrating percent survival of young and aged Balb/cBy mice intranasally challenged with 10^7 and 10^6 CFU of *S. pneumoniae* (WT: 10^7 young $n = 13$, 10^7 aged $n = 13$, 10^6 young $n = 6$, 10^6 aged $n = 6$) and an isogenic PsrP-deficient mutant. (*ΔpsrP*: 10^7 young $n = 6$, 10^7 aged $n = 6$, 10^6 young $n = 6$, 10^6 aged $n = 6$). Both young and aged mice challenged with 10^6 Δ*psrP* had significantly improved survival vs. WT-infected mice. Statistical analysis was performed using a Kaplan–Meier log-rank Test. (B) Bacterial burden in the lungs and blood of young and aged mice sacrificed 2 days following intratracheal administration of 10^5 CFU of WT and *ΔpsrP* pneumococci ($n = 6$ per group). Note that mice infected with the PsrP-deficient strain do not demonstrate an age-dependent increase in bacterial titers vs. WT. Asterisks denote a statistical significant difference when using one-way ANOVA (Duncan's Method; $P < 0.05$).

cells or normal cells exposed to SASP is one mechanism by which the lungs of the elderly and patients with COPD may be primed for infection by numerous pathogens.

Between young and aged mice and in humans, the most dramatic difference in ligand levels that we observed was in regard to K10. Increased survival of aged mice infected with a PsrP-deficient mutant demonstrated the importance of this host–ligand interaction for severe pneumococcal disease. Unlike LR or PAFr, which are ubiquitously expressed, K10 is found predominantly in differentiated keratinocytes and on mucosal epithelial cells of the lungs and nares (Paramio *et al.*, 2001; O'Brien *et al.*, 2002; Shivshankar *et al.*, 2009). Thus, the contribution of elevated K10 to infection is most likely limited to the lungs and not during sepsis or meningitis. Of note, passive and active immunization with PsrP has been shown to be protective against challenge in young mice (Rose *et al.*, 2008; Shivshankar *et al.*, 2009). This indicates that vaccines designed for the use in the elderly might be optimized to neutralize the activity of bacterial adhesins that target age-dependent inflammation-regulated ligands on host cells, such as K10.

We observed that induction of senescence with bleomycin enhanced K10 expression in alveolar epithelial cells *in vitro*. Because K10 expression has been shown to result in pRb activation and cell cycle arrest (Paramio *et al.*, 1999, 2001), this observation suggests that K10 may be involved in a positive-feedback loop with pRb that together leads to epithelial cell senescence. Further studies are warranted to examine this possibility. Induction of genotoxic stress with H_2O_2 and bleomycin corroborated the role of cellular senescence in susceptibility of live animals to infection but was obfuscated by the pleiotropic effects of these genotoxic agents. Although administration of H_2O_2 results in generalized oxidative stress and bleomycin causes lung fibrosis, exposure to nonspecific genotoxic stress occurs during smoking and possibly explains the high incidence of cellular senescence in the lungs of individuals with COPD (Aoshiba *et al.*, 2003; Aoshiba & Nagai, 2009).

At this time, it not possible to block the development of cellular senescence in aged mice. Thus, a direct cause and effect relationship between senescent cells and the susceptibility of aged animals to pneumonia could not be demonstrated. While multiple factors were potentially involved in the increased susceptibility of aged mice to pneumonia, our observation of increased expression of p16, pRb and mH2A, enhanced lung inflammation, increased bacterial attachment to senescent cells and normal cells exposed to senescent media, and the enhanced susceptibility of aged mice to infection in a PsrP-dependent manner are strong correlative findings that support the hypothesis that senescent cells prime the lungs for pneumonia through increased bacterial adhesion. These findings clearly suggest that cellular senescence impacts inflammation and infectious disease in the lungs and provide an additional molecular explanation for the increased incidence of CAP in the elderly and those with COPD.

Experimental procedures

All animal experiments and those with de-identified human tissues were reviewed and approved by the appropriate University of Texas Health Science Center institutional review board.

Collection and processing of lung samples

Young (4–5 months) and aged (19–22 months) female Balb/cBy mice were obtained from the National Institute on Aging Aged Rodent Colony and housed in ABSL-1 facilities. Following their asphyxiation with isoflurane, lungs were excised, washed with sterile phosphate-buffered saline (PBS), and processed for paraffin embedding and collection of whole-lung homogenates. Human lung samples were obtained from the Lung Tissue Research Consortium (LTRC) sponsored by National Heart, Lung and Blood Institute. Frozen tissue blocks were obtained from young (43–50 years), mature (51–64 years), and elderly (65–82 years) individuals during lung biopsy sample collection or surgical resection. Only normal tissues as determined by pathological examination by LTRC staff were used. Paraffin-embedded lungs were sectioned at 5 μm thickness and stained with hematoxylin and eosin for pathological examination. Five lung sections from each mouse were scored on a 1–5 scale on the basis of peribronchial, perivascular, and intraalveolar inflammation, interstitial pneumonitis, and thickening of the alveolar walls. Unstained sections were utilized for immunohistochemical analyses as described later.

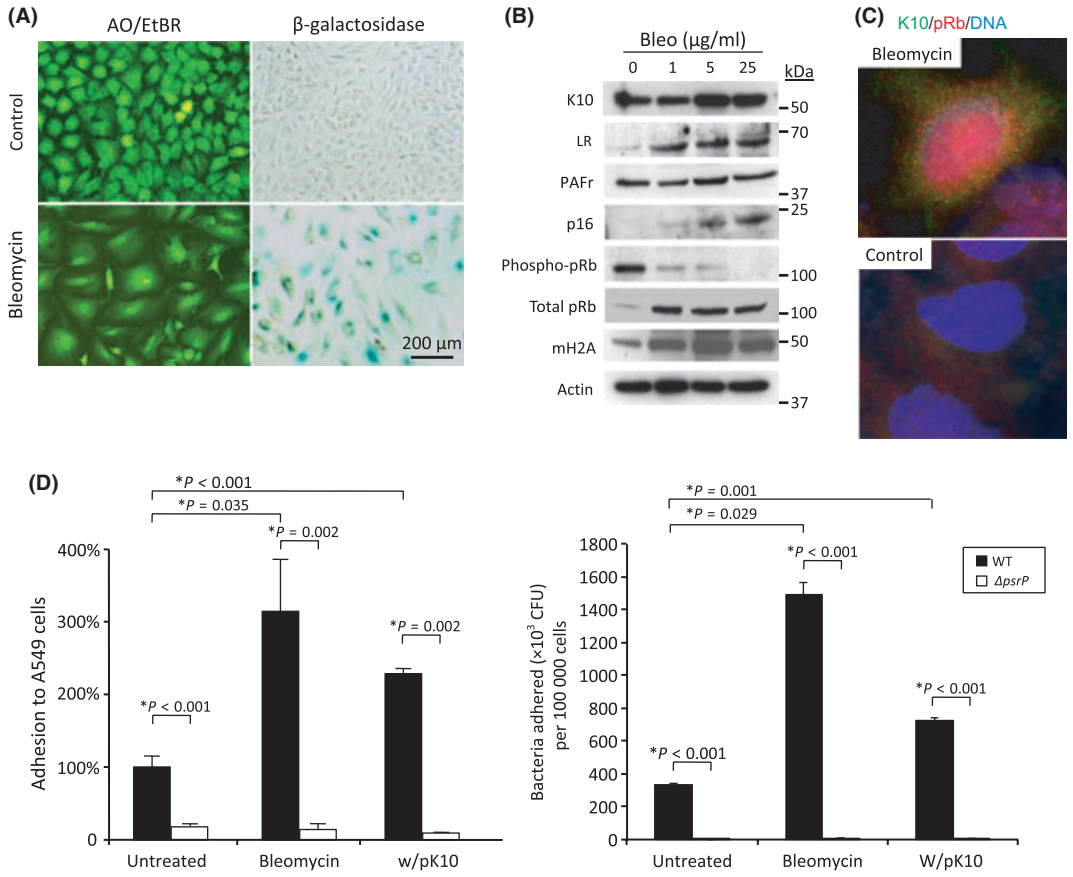

Fig. 5 Senescent lung cells express enhanced levels of pneumococcal ligands and are permissive for bacterial adhesion *in vitro*. A549 type II alveolar epithelial cells were pulsed with bleomycin to induce cellular senescence. We observed that after 8 days, almost all cells had (A) characteristic cell flattening and increased senescence-associated β-galactosidase activity when treated with 25 μg mL^{-1} bleomycin. (B) Western blot analysis for the pneumococcal ligands K10, laminin receptor, and PAFr as well as the senescence markers p16, pRb, and mH2A in bleomycin-pulsed A549 cells. (C) Immunofluorescent detection of pRb and K10 showing nuclear localization of pRb with increased expression of K10 in bleomycin-pulsed A549 cells. (D) Adhesion of wild-type *S. pneumoniae* (WT) and the PsrP-deficient mutant (*ΔpsrP*) to bleomycin-treated A549 cells. K10-transfected cells were included as a positive control. Given the substantial difference in cell size between normal and senescent cells, the same experimental data are represented in as the percent increase in bacterial adhesion to confluent monolayers with equal surface area (i.e., 2.0 cm^2) and as the number of pneumococci adhered per 100 000 cells. Asterisks denote a statistical significant difference when using a two-tailed Student's *t*-test.

Analysis of proinflammatory cytokine production

Cytokine levels in tissue homogenates were determined by ELISA using IL-1α, IL-1β, IL-6, TNFα, and CXCL1 kits from BD Pharmingen. Levels of IL-1β, IL-6, IL-8, IL-10, IL-12p70, and TNFα in A549 cell supernatants were determined using a BDCytometric Bead Array (CBA) Human Inflammatory Cytokines Kit. Levels of IL-1α produced by these cells were determined using a human IL-1α ELISA kit (R&D Systems, Minneapolis, MN, USA).

Immunoblotting

Whole-lung homogenates and A549 cell lysates were prepared in appropriate volumes of RIPA buffer, and the protein concentration was determined using the bicinchoninic acid assay. Immunoblotting was carried out with 10–15 μg protein per sample using standard protocols. Primary antibodies used included rabbit anti-human K10 (Epitomics, Burlingame, CA, USA), mouse anti-human LR (Abcam), rabbit anti-human PAFr (Cayman Chemicals, Ann Arbor, MI, USA), rabbit anti-human actin (Abcam), mouse anti-human pRb (Cell Signaling, Danverse, MA, USA), rabbit anti-mouse pRb (Cell Signaling), rabbit anti-phospho-pRb (Cell Signaling, Danverse, MA, USA), rabbit anti-human p16 (Santa Cruz Biotechnology, Santa Cruz, CA, USA), and rabbit anti-histone mH2A1 (Millipore, Billerica, MA, USA). Primary antibodies were shown by the manufacturer to cross-react with both mouse and human orthologues except for pRb. All antibodies were used at a minimal dilution of 1:500.

Semiquantitative analyses of immunoblots

Relative protein levels were determined by comparative densitometric analysis of Western blot bands using a Molecular Imager Gel Doc XR System (BioRad, Hercules, CA, USA). For each protein examined, the membrane initially probed was stripped, and the amount of actin was determined using rabbit anti-actin antibodies (Bethyl laboratories, Inc., Montgomery, TX, USA). Relative levels of protein were determined by dividing the intensity of the tested protein band to that of actin within the same lane and membrane.

Immunohistochemistry for K10

Paraffin-embedded lung sections were deparaffinized with xylene and rehydrated using an ethanol gradient. Following rinsing with PBS, the

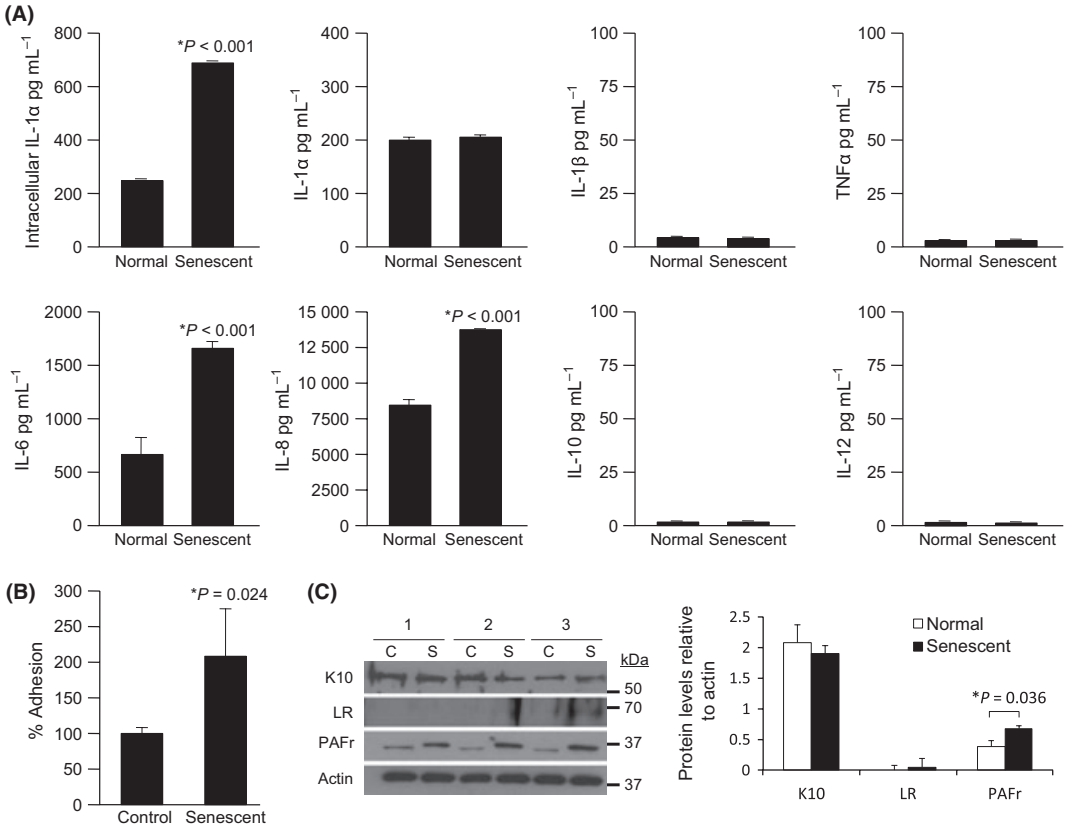

Fig. 6 Normal A549 cells exposed to conditioned media from senescent cells are permissive for bacterial adhesion. (A) Proinflammatory cytokine profile of senescent A549 cells (n = 3, with duplicate wells per experiment). Intracellular IL-1α as well as secreted IL-1α, IL-1β, TNFα, IL-6, IL-8, IL-10, and IL-12 produced by senescent and normal A549 cells was measured 8 days after a 24-h pulse with 10 μg mL^{-1} bleomycin or mock, respectively, using a cytometric bead array. (B) Mean relative adhesion of *S. pneumoniae* to A549 cells exposed to either conditioned media from normal or senescent A549 cells for 2 h. Experiments were performed in triplicate. For panels A and B, asterisks denote a statistical significant difference when using a two-tailed Student's *t*-test. (C) Western blots and corresponding densitometric analyses for K10, laminin receptor, and PAFr levels in A549 cells exposed to conditioned media after 2 h. Samples were collected from three independent experiments, from either control (C) or bleomycin-induced senescent cells (S). Histogram shows composite densitometric data (protein/actin) with actin probed from the same lanes and membrane as the tested protein. The representative actin blot corresponds to the PAFr immunoblot.

sections were treated with 0.3% H_2O_2 in 100% methanol to quench endogenous peroxidase activity. Slides were rinsed twice with PBS then submerged in 4% paraformaldehyde for 20 min at room temperature. Sections were washed twice with PBS then microwaved twice in Target Unmasking Fluid (Invitrogen) for 5 min with a 1-min interval. After cooling in room temperature water, tissue sections were blocked with 10% FBS in PBS for 1 h at room temperature. The sections were then incubated with antibody against K10 (1:40) at 4 °C overnight. Sections were washed thrice with PBS and incubated with goat anti-rabbit IgG conjugated to HRP (1:200 dilution) for 1 h at room temperature. The slides were washed four times then stained with the DAB substrate kit following the manufacturer's protocol (BD Parmingen). Following color development, slides were rinsed with water then counterstained for 2 min with hematoxylin. Sections were dehydrated and cover slipped using standard protocols. For each mouse (n = 5 per age group), two lung sections were examined using a light microscope at a magnification of 400X. Images were captured and processed using Leica software.

Infection of mice with *S. pneumoniae*

Streptococcus pneumoniae, serotype 4 strain TIGR4 and T4Δ*psrP*, a previously described isogenic mutant deficient in *psrP*, were grown on blood agar plates or in Todd Hewitt broth (THB) at 37 °C in 5% CO_2 (Obert *et al.*, 2006; Rose *et al.*, 2008). Erythromycin (1 μg mL^{-1}) was added to the culture media to maintain the *psrP* mutation. Bacterial cultures were grown to mid-logarithmic phase (OD_{620} = 0.5), pelleted by centrifugation, and suspended in sterile PBS. For assessment of the contribution of PsrP/K10 to age-dependent disease severity, mice were infected intranasally with 10^7 and 10^6 CFU of TIGR4 or T4Δ*psrP* in a 25-μl suspension. Mortality over 10 days was assessed. To determine age-related changes in bacterial titers, a parallel set of mice were inoculated intratracheally with 10^5 CFU in 100 μL PBS. Two days postchallenge, mice were sacrificed and the lungs and blood were collected. Bacterial titers in the lungs and blood were determined by plating serial dilutions of the lung homogenate or blood and extrapolation from colony counts following overnight incubation. All animal infection studies were conducted in ABSL-2 facilities.

Induction of cellular senescence *in vitro*

A549 (ATCC CRL-185) cells were maintained in F12 medium supplemented with 10% fetal bovine serum and antibiotics. A549 cells were pulsed with 0–25 μg mL^{-1} bleomycin sulfate for 1 day then washed and maintained in fresh culture medium for 8 days. Cellular senescence was confirmed by the detection of senescence-associated β-galactosidase activity (Dimri *et al.*, 1995; Debacq-Chainiaux *et al.*, 2009).

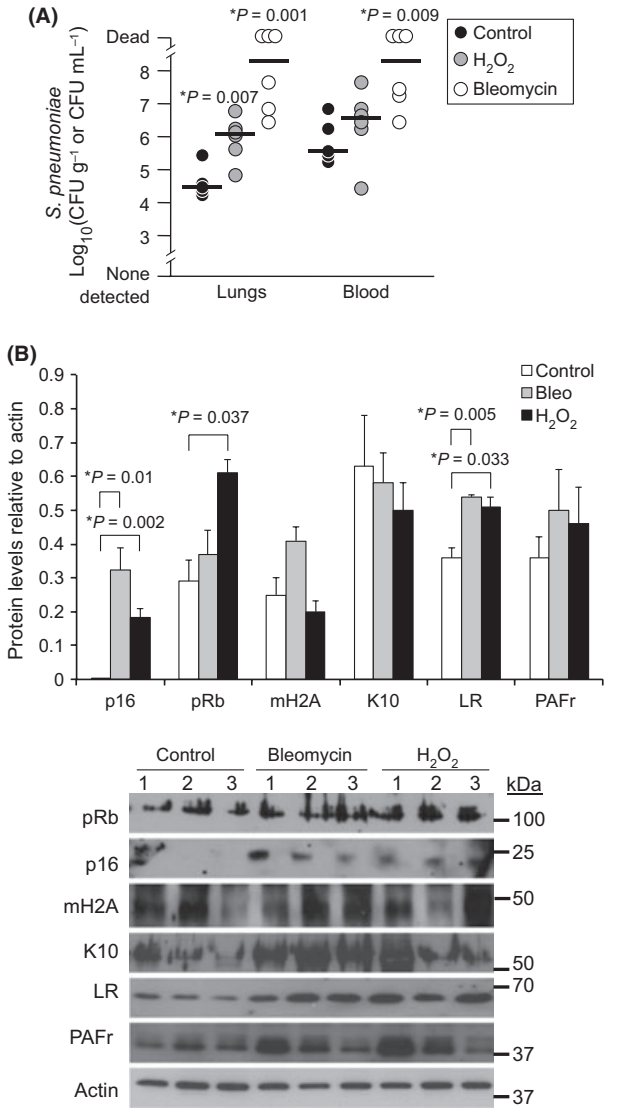

Fig. 7 Genotoxic stress enhances susceptibility to pneumonia and is positively correlated with increased bacterial ligand expression. (A) Bacterial titers in the lungs and blood of mice 2 days after challenge with *S. pneumoniae* ($n = 6$ per cohort). Mice had been intratracheally administered saline (Control), saline with bleomycin (Bleo) at 0.033 mg kg^{-1} body weight 3 weeks prior or had their drinking water supplemented with 0.5% hydrogen peroxide for 3 weeks (H_2O_2). Asterisks denote a statistical significant difference ($P < 0.05$). Statistical analyses were performed using a two-tailed Student's *t*-test. (B) Western blot analysis for the senescence markers pRb, p16, and mH2A, as well as pneumococcal ligands K10, laminin receptor, and PAFr using whole-lung homogenates from control, Bleo, and H_2O_2-administered animals.

Immunofluorescence assay

Detection of pRb and K10 was made as described previously (Shivshankar *et al.*, 2009) with brief modifications. Eight days after, control or bleomycin-pulsed A549 cells grown on coverslips were washed and fixed in 4% paraformaldehyde for 20 min at room temperature. Cells were permeabilized with 0.1% triton-X-100 for 5 min and blocked in 10% FBS-containing F12 medium for 1 h at room temperature. Primary antibodies for pRb (mouse anti-human pRb) and K10 (rabbit anti-human K10) were added at 1:100 dilution and incubated at 4 °C overnight. Cells were washed with PBS thrice for 5 min and incubated with goat anti-mouse IgG PE and goat anti-rabbit FITC (1:200 dilution) to detect pRb and K10, respectively, along with DAPI for nuclear staining for 1 h at room temperature. Cells were washed and coverslips mounted on glass slides using Fluorsave mounting solution (Merck Biosciences, Darmstadt, Germany). Fluorescent staining in the cells was observed using Olympus AX-70 Fluorescence microscope, and images were acquired using a Hamamatsu digital camera. All single-color images were then superimposed and processed with the software SimplePCI to display multicolors.

Adhesion assays

Bacterial adhesion assays were performed using protocols previously described (Rose *et al.*, 2008; Shivshankar *et al.*, 2009). Exponential cultures of *S. pneumoniae* were pelleted and suspended in PBS at 10^7 CFU mL^{-1} ($OD_{620} = 0.1$) and added to confluent monolayers of control and bleomycin-pulsed A549 in a 24-well plate (2.0 cm^2). After 1-h incubation at 37 °C, cells were washed gently with PBS thrice to remove unattached bacteria, lysed with 0.1% Triton-X-100 in PBS, and the lysate was plated on blood agar plates and incubated for extrapolation of attached bacteria from the number of colonies. Transiently transfected A549 cells with pCDNA-K10 were used as positive controls to compare the effect of bleomycin on pneumococcal adhesion (Paramio *et al.*, 1999; Shivshankar *et al.*, 2009). Adhesion assays were performed at minimum in triplicate with three wells per condition tested in each experiment. Because of the difference in cell size between normal and senescent cells, bacterial adhesion data are presented as the percent adhesion relative to WT-infected untreated cell monolayers (i.e., equal surface area), likewise, as the number of attached bacteria per 100 000 A549 cells. To determine the latter, monolayers were trypsinized and cells were counted using a Neubauer hemocytometer. For analysis of the paracrine effect of senescent cells on adhesion cell culture, supernatants from control and bleomycin-treated A549 cells after 8 days were applied to fresh monolayer of A549 cells for 2 h prior to the addition of bacteria.

Induction of genotoxic stress

Bleomycin sulfate at 0.033 mg kg^{-1} body weight was administered intratracheally to 4- to 5-month-old female Balb/cJ following the protocol described by Aoshiba *et al.* (Aoshiba *et al.*, 2003). Control animals were administered sterile PBS, which was used as the bleomycin vehicle. Three weeks later, mice were used for experimental purposes. Alternatively, oxidative stress was induced using the protocol previously described by Weiner *et al.* (Weiner *et al.*, 2000). Briefly, mice were given drinking water supplemented with 0.5% H_2O_2 *ad libitum* for 3 weeks prior to their experimental use.

Statistical analysis

For statistical comparisons between two cohorts, a two-tailed Student's *t*-test was used. For the comparison of bacterial burden between young and aged mice challenged with wild-type and mutant *S. pneumoniae*, a one-way ANOVA (Duncan's test) was used. For the analysis of survival following bacteria challenge, a Kaplan–Meier log-rank test was employed. All statistical analyses were performed using *SigmaStat* software (Systat Software).

Role of funding source

The funding sources had no involvement in study design, in the collection, analysis, and interpretation of the data, or in the writing of the report.

Acknowledgments

We thank Benjamin J. Daniel for assistance with cytometric analyses. For CJLS, this work was supported by the Leahi Foundation. For CJO, this work was supported by the National Institute for Health grants AG092313, AG033274 and AI078972.

Conflict of interest

None of the authors have a conflict of interest.

References

Aoshiba K, Nagai A (2009) Senescence hypothesis for the pathogenetic mechanism of chronic obstructive pulmonary disease. *Proc. Am. Thorac. Soc.* **6**, 596–601.

Aoshiba K, Tsuji T, Nagai A (2003) Bleomycin induces cellular senescence in alveolar epithelial cells. *Eur. Respir. J.* **22**, 436–443.

Avadhanula V, Rodriguez CA, Ulett GC, Bakaletz LO, Adderson EE (2006) Nontypeable *Haemophilus influenzae* adheres to intercellular adhesion molecule 1 (ICAM-1) on respiratory epithelial cells and upregulates ICAM-1 expression. *Infect. Immun.* **74**, 830–838.

Barbier M, Oliver A, Rao J, Hanna SL, Goldberg JB, Alberti S (2008) Novel phosphorylcholine-containing protein of *Pseudomonas aeruginosa* chronic infection isolates interacts with airway epithelial cells. *J. Infect. Dis.* **197**, 465–473.

Campisi J (2005) Senescent cells, tumor suppression, and organismal aging: good citizens, bad neighbors. *Cell* **120**, 513–522.

Campisi J, d'Adda di Fagagna F (2007) Cellular senescence: when bad things happen to good cells. *Nat. Rev. Mol. Cell Biol.* **8**, 729–740.

Conners R, Hill DJ, Borodina E, Agnew C, Daniell SJ, Burton NM, Sessions RB, Clarke AR, Catto LE, Lammie D, Wess T, Brady RL, Virji M (2008) The Moraxella adhesin UspA1 binds to its human CEACAM1 receptor by a deformable trimeric coiled-coil. *EMBO J.* **27**, 1779–1789.

Coppe JP, Patil CK, Rodier F, Sun Y, Munoz DP, Goldstein J, Nelson PS, Desprez PY, Campisi J (2008) Senescence-associated secretory phenotypes reveal cell-nonautonomous functions of oncogenic RAS and the p53 tumor suppressor. *PLoS Biol.* **6**, 2853–2868.

Coppe JP, Desprez PY, Krtolica A, Campisi J (2009) The senescence-associated secretory phenotype: the dark side of tumor suppression. *Annu. Rev. Pathol.* **5**, 99–118.

Cundell DR, Gerard NP, Gerard C, Idanpaan-Heikkila I, Tuomanen EI (1995) *Streptococcus pneumoniae* anchor to activated human cells by the receptor for platelet-activating factor. *Nature* **377**, 435–438.

Debacq-Chainiaux F, Erusalimsky JD, Campisi J, Toussaint O (2009) Protocols to detect senescence-associated beta-galactosidase (SA-betagal) activity, a biomarker of senescent cells in culture and *in vivo*. *Nat. Protoc.* **4**, 1798–1806.

Dimri GP, Lee X, Basile G, Acosta M, Scott G, Roskelley C, Medrano EE, Linskens M, Rubelj I, Pereira-Smith O, Peacocke M, Campisi J (1995) A biomarker that identifies senescent human cells in culture and in aging skin *in vivo*. *Proc. Natl. Acad. Sci. U S A* **92**, 9363–9367.

Garcia CK, Wright WE, Shay JW (2007) Human diseases of telomerase dysfunction: insights into tissue aging. *Nucleic Acids Res.* **35**, 7406–7416.

Hinojosa E, Boyd AR, Orihuela CJ (2009) Age-associated inflammation and toll-like receptor dysfunction prime the lungs for pneumococcal pneumonia. *J. Infect. Dis.* **200**, 546–554.

Kinsella K, Velkoff VA (2001) *An Aging World: 2001*. (USC Bureau, ed.). Washington, DC: U.S. Goverment Printing Office.

Kline KA, Falker S, Dahlberg S, Normark S, Henriques-Normark B (2009) Bacterial adhesins in host-microbe interactions. *Cell Host Microbe.* **5**, 580–592.

Kreiling JA, Tamamori-Adachi M, Sexton AN, Jeyapalan JC, Munoz-Najar U, Peterson AL, Manivannan J, Rogers ES, Pchelintsev NA, Adams PD, Sedivy JM (2011) Age-associated increase in heterochromatic marks in murine and primate tissues. *Aging Cell* **10**, 292–304.

Krtolica A, Campisi J (2002) Cancer and aging: a model for the cancer promoting effects of the aging stroma. *Int. J. Biochem. Cell Biol.* **34**, 1401–1414.

Lexau CA, Lynfield R, Danila R, Pilishvili T, Facklam R, Farley MM, Harrison LH, Schaffner W, Reingold A, Bennett NM, Hadler J, Cieslak PR, Whitney CG (2005) Changing epidemiology of invasive pneumococcal disease among older adults in the era of pediatric pneumococcal conjugate vaccine. *JAMA* **294**, 2043–2051.

Lopez AD, Mathers CD, Ezzati M, Jamison DT, Murray CJ (2006) Global and regional burden of disease and risk factors, 2001: systematic analysis of population health data. *Lancet* **367**, 1747–1757.

Meyer KC, Ershler W, Rosenthal NS, Lu XG, Peterson K (1996) Immune dysregulation in the aging human lung. *Am. J. Respir. Crit. Care Med.* **153**, 1072–1079.

Meyer KC, Rosenthal NS, Soergel P, Peterson K (1998) Neutrophils and low-grade inflammation in the seemingly normal aging human lung. *Mech. Ageing Dev.* **104**, 169–181.

Obert C, Sublett J, Kaushal D, Hinojosa E, Barton T, Tuomanen EI, Orihuela CJ (2006) Identification of a candidate *Streptococcus pneumoniae* core genome and regions of diversity correlated with invasive pneumococcal disease. *Infect. Immun.* **74**, 4766–4777.

O'Brien LM, Walsh EJ, Massey RC, Peacock SJ, Foster TJ (2002) *Staphylococcus aureus* clumping factor B (ClfB) promotes adherence to human type I cytokeratin 10: implications for nasal colonization. *Cell Microbiol.* **4**, 759–770.

Orihuela CJ, Fogg G, DiRita VJ, Tuomanen E (2005) Bacterial interactions with mucosal epithelial cells. in *Mucosal Immunology* (Mestecky J, Lamm ME, Strober W, Bienenstock J, McGhee JR, Mayer L, eds). Burlington, MA: Elsevier Academic Press, pp. 753–767.

Orihuela CJ, Mahdavi J, Thornton J, Mann B, Wooldridge KG, Abouseada N, Oldfield NJ, Self T, Ala'Aldeen DA, Tuomanen EI (2009) Laminin receptor initiates bacterial contact with the blood brain barrier in experimental meningitis models. *J. Clin. Invest.* **119**, 1638–1646.

Paramio JM, Casanova ML, Segrelles C, Mittnacht S, Lane EB, Jorcano JL (1999) Modulation of cell proliferation by cytokeratins K10 and K16. *Mol. Cell. Biol.* **19**, 3086–3094.

Paramio JM, Segrelles C, Ruiz S, Jorcano JL (2001) Inhibition of protein kinase B (PKB) and PKCzeta mediates keratin K10-induced cell cycle arrest. *Mol. Cell. Biol.* **21**, 7449–7459.

Paterson GK, Orihuela CJ (2010) Pneumococcal microbial surface components recognizing adhesive matrix molecules targeting of the extracellular matrix. *Mol. Microbiol.* **77**, 1–5.

Rose L, Shivshankar P, Hinojosa E, Rodriguez A, Sanchez CJ, Orihuela CJ (2008) Antibodies against PsrP, a novel *Streptococcus pneumoniae* adhesin, block adhesion and protect mice against pneumococcal challenge. *J. Infect. Dis.* **198**, 375–383.

Shivshankar P, Sanchez C, Rose LF, Orihuela CJ (2009) The *Streptococcus pneumoniae* adhesin PsrP binds to Keratin 10 on lung cells. *Mol. Microbiol.* **73**, 663–679.

Swords WE, Buscher BA, Ver Steeg Ii K, Preston A, Nichols WA, Weiser JN, Gibson BW, Apicella MA (2000) Non-typeable *Haemophilus influenzae* adhere to and invade human bronchial epithelial cells via an interaction of lipooligosaccharide with the PAF receptor. *Mol. Microbiol.* **37**, 13–27.

Tsuji T, Aoshiba K, Nagai A (2010) Alveolar cell senescence exacerbates pulmonary inflammation in patients with chronic obstructive pulmonary disease. *Respiration* **80**, 59–70.

Weiner ML, Freeman C, Trochimowicz H, de Gerlache J, Jacobi S, Malinverno G, Mayr W, Regnier JF (2000) 13-week drinking water toxicity study of hydrogen peroxide with 6-week recovery period in catalase-deficient mice. *Food Chem. Toxicol.* **38**, 607–615.

WHO (2009) *Chronic Obstructive Pulmonary Disease (COPD)*. (WM centre, eds). World Health Organization.

Yende S, Tuomanen EI, Wunderink R, Kanaya A, Newman AB, Harris T, de Rekeneire N, Kritchevsky SB (2005) Preinfection systemic inflammatory markers and risk of hospitalization due to pneumonia. *Am. J. Respir. Crit. Care Med.* **172**, 1440–1446.

Supporting Information

Additional supporting information may be found in the online version of this article:

Fig. S1 Pro-inflammatory cytokine profile of young mice with induced genotoxic stress.

As a service to our authors and readers, this journal provides supporting information supplied by the authors. Such materials are peer-reviewed and may be re-organized for online delivery, but are not copy-edited or typeset. Technical support issues arising from supporting information (other than missing files) should be addressed to the authors.